Radial Cracks in Perforated Thin Sheets

Romain Vermorel, Nicolas Vandenberghe,* and Emmanuel Villermaux†
IRPHE, Aix Marseille Université–CNRS, 13384 Marseille Cedex 13, France
(Received 24 January 2010; published 30 April 2010)

When a rigid cone is slowly pushed through a thin elastic sheet, the material breaks, exhibiting a network of cracks expanding in the radial direction. Experiments conducted with aluminum sheets show that the number of cracks is selected at the beginning of the perforation process and then remains stable. A simple model predicts the number of cracks as the result of a competition between the elastic energy stored in the sheet, and the energy dissipated during crack extension. We also evidence the subtle rearrangements of randomly distributed cracks into uniform radial patterns with fewer cracks. In that respect, this study exemplifies how relaxation mechanisms in fragmenting solids can attenuate the influence of defects in the material.

DOI: 10.1103/PhysRevLett.104.175502 PACS numbers: 62.20.mt, 46.50.+a, 46.70.Hg

Broken windows [1,2], ice layers [3], and impacted metal plates [4] often exhibit radial cracks after perforation, patterns which are also observed on coated elastic materials [5] or in drying suspension [6]. Most of the work dealing with the occurrence of cracks under localized transverse load have emphasized the threshold at which the material breaks. However, in a number of applications related to fragmentation, the size of the fragments and thus the pattern of cracks that develops after the onset of breaking is of prime interest [7]. The present Letter investigates the radial crack patterns observed in thin sheets perforated quasistatically by a rigid cone. Our analysis emphasizes the geometry of the rupture patterns as well as the underlying mechanisms of their selection and rearrangements. We do not discuss the detailed and complex conditions under which cracks initiate and propagate but rather develop a simple approach based on the competition between surface creation and elastic energy stored in the material to explain how the pattern is selected.

We use annular thin sheets cut out of aluminum foil (Young's modulus $E = 70$ GPa, Poisson ratio $\nu = 0.3$, thickness $h = 18$ μm). The foil is clamped at its outer radius ($R_s = 60$ mm) with no pretension. A rigid cone, whose axis is perpendicular to the sheet and intersects it at its center is mounted on a translation stage (Fig. 1). The direction of translation coincides with the axis of the cone, which is incrementally (increment size $\delta z = 0.1$ mm) pushed to enlarge the initial hole in the sheet. It does so by opening radial cracks. Two cones, with different angles (20° and 45°) were used leading to the same results. The penetration radius R is measured at the intersection of the cone and the plane of the sheet. The circular inner edge, of radius $R_0 = 1.5$ mm, prevents the sheet from breaking dynamically at the early stage of the process, as would an intact sheet punctured by the sharp tip of the cone. Thus, the perforation can be considered to be quasistatic. We have also performed experiments with an imposed initial uniform pattern of n_0 cracks, each of initial length 1.5 mm, to study the rearrangements of the radial crack network with increasing penetration depth.

Figure 2(a) shows the number of cracks obtained with a different initial number of cracks n_0. The number of cracks is measured at $R = 25$ mm and does not change for larger R. For $n_0 \leq 4$, the number of radial cracks increases through the initiation of new cracks or branching of the previous ones as shown on Fig. 2(b). The pattern systematically evolves toward a uniform radial crack network. However, for a few experiments with $n_0 = 4$, the pattern does not expand radially but spontaneously starts to rotate to form spiraling cracks [8]. This behavior is not observed for other values of n. For $5 \leq n_0 \leq 12$, the initial number of cracks is conserved and we observe uniform patterns of $n = n_0$ cracks expanding in the radial direction. For larger values of n_0 ($n_0 \geq 13$), the number of cracks decreases so that $n \leq n_0$. In that regime n does not depend on n_0 and the

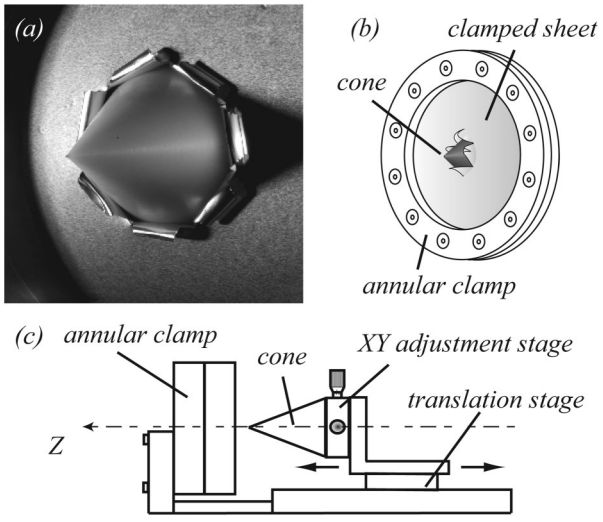

FIG. 1. (a) Picture of the cone perforating the aluminum sheet. (b) Clamped sheet. (c) Sketch of the experimental setup used for perforation.

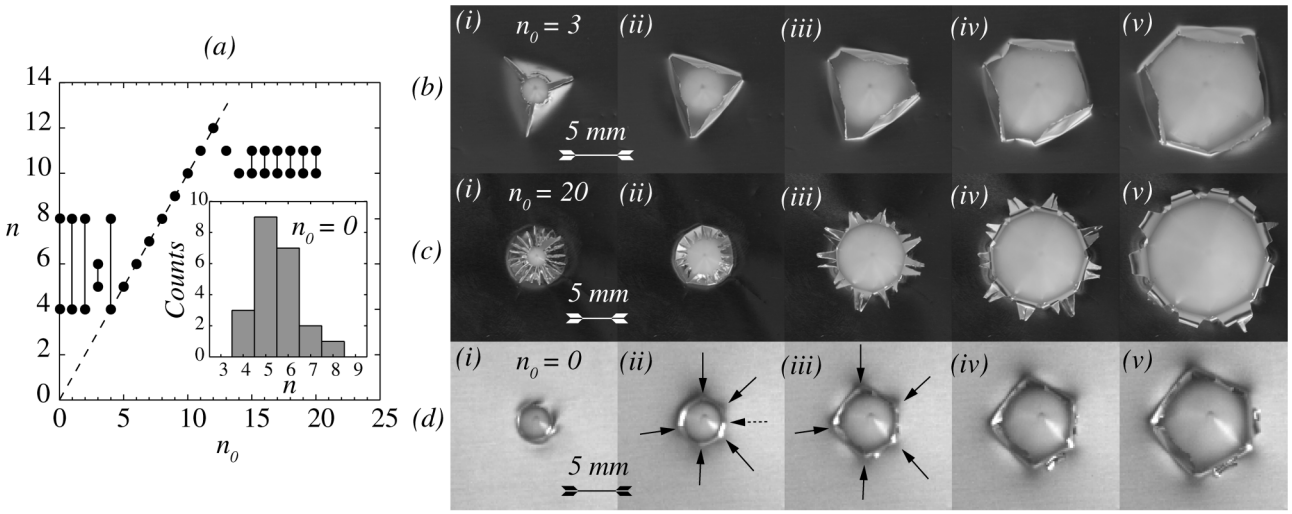

FIG. 2. (a) Number of cracks n obtained for different initial numbers n_0. At a given n_0, the solid lines emphasize the dispersion of the results. The inserted figure shows the distribution of crack numbers for $n_0 = 0$. (b)–(d) Evolution of the pattern for (b) $n_0 = 3$; (c) $n_0 = 20$; (d) $n_0 = 0$. The penetration depth increases from left to right by steps of 1.5 mm, 2.4 mm, and 1 mm for (b), (c), and (d), respectively. In (d), the arrows point to the cracks and the dashed line arrow shows a crack which does not further expand with increasing penetration depth.

final number systematically decreases to $n = 10$ or $n = 11$. Figure 2(c) shows how the pattern rearranges from $n_0 = 20$ to $n = 10$ over a few increments δz. With no initial cracks [inset in Fig. 2(a)], the most probable number of cracks is $n = 5$, with some dispersion. Figure 2(d) illustrates an experiment starting from $n_0 = 0$ and leading to a final number $n = 5$. Interestingly, we observe the rearrangement of the pattern switching from $n = 6$ to $n = 5$ cracks between pictures (ii) and (iii): the dashed line arrow points to a crack for which the local configuration was similar to the case of large n_0 and, as a result, this crack did not further expand.

To compute the strain and stress fields in the sheet as the cone penetrates, we consider that the problem is planar. We neglect bending energy because the thickness of the sheet is small ($h/R \sim 10^{-3}$), so that the energy required to fold a petal between two adjacent cracks is negligible [9]. Figure 3(a) shows a schematic of the inner boundary of the sheet, for a uniform pattern of n radial cracks. The initially straight segment $[CC']$ joining two crack tips, is stretched to a length equal to $2(AB + BC)$ as the cone is forced through the sheet. We express the corresponding extensional strain ϵ_n in terms of n and ϕ_n the angle between the tangent to the cone and $[CC']$

$$\epsilon_n = \frac{\phi_n \cos(\pi/n - \phi_n) + \sin(\pi/n - \phi_n)}{\sin(\pi/n)} - 1. \quad (1)$$

The angle ϕ_n, which determines the position of the crack tips is bounded by two limits: if $\phi_n = 0$, the crack tips are localized at maximum distance of the cone and the sheet is stress free ($\epsilon_n = 0$); if $\phi_n = \pi/n$, the crack tips are in contact with the cone and then, the strain is maximum $[\tilde{\epsilon}_n = (\pi/n)/\sin(\pi/n) - 1]$.

We assume that the sheet is made of a perfect elastic material; i.e., we neglect plastic deformation that we consider to be confined to a small area of the membrane with a limited effect on the total energy. To compute the stored elastic energy, we replace the complex inner shape of the membrane by a circular edge at radius R with azimuthal strain ϵ_n yielding the radial displacement field $\zeta(r) = R_s R^2 (R_s^2 - R^2)^{-1} (R_s/r - r/R_s)\epsilon_n$ [10]. The strains are $\epsilon_r = \partial\zeta/\partial r$ and $\epsilon_\theta = \zeta/r$ and the stresses are given by Hooke's law. The stress σ_θ is positive in the vicinity of the cone, and this tension leads to further extension of the cracks. The stretching energy $U_e = \pi h \int (\sigma_r \epsilon_r + \sigma_\theta \epsilon_\theta) r dr$ of the annular membrane clamped at R_s with imposed azimuthal strain ϵ_n at R writes

$$U_e = \frac{\pi \epsilon_n^2}{1 - \nu^2} \left((1 - \nu)\frac{R_s^2}{R^2} + 1 + \nu \right) \frac{EhR^4}{R_s^2 - R^2}. \quad (2)$$

To predict the crack length, we resort to the celebrated Griffith's criterion [11]. The energy needed to create new surface δU_c must be balanced by the change of bulk elastic energy stored in the material δU_e. The irreversibility at the microscopic level during crack growth may be taken into account by introducing a fracture energy Γ which embraces the energy required to break material bonds as well as other dissipative processes localized near the crack tip. Increasing crack length by δL thus requires an energy $\delta U_c = 2\Gamma h \delta L$. For $\delta L = n\delta l$, in which δl is the incremental length of a single crack, Griffith's criterion takes the form

$$\frac{\delta U}{\delta L} = \frac{\delta(U_e + U_c)}{\delta L} = 0 \Rightarrow \frac{\delta U_e}{\delta l} = -2n\Gamma h. \quad (3)$$

Noticing that $\delta U_e/\delta l = (\delta U_e/\delta \phi_n)(\delta \phi_n/\delta l)$, further geometric considerations provide

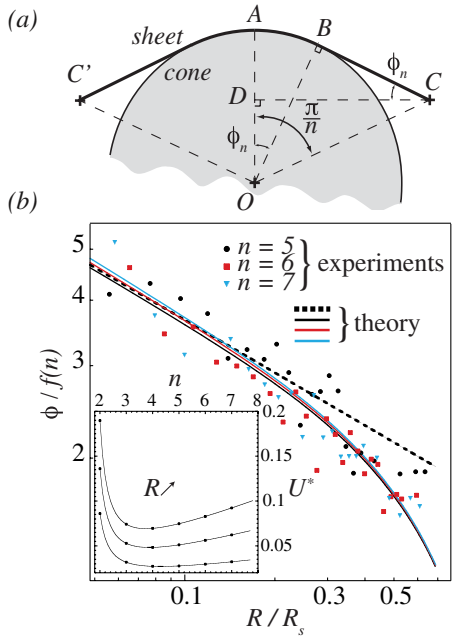

FIG. 3 (color online). (a) Schematic of the deformation of the inner boundary of the sheet in contact with the cone between crack tips located in C and C'. The folded petal is not shown. (b) Evolution of the angle $\phi_n/f(n)$ with the perforation radius R/R_s. The solid line stands for the full theoretical prediction and the dotted line represents the approximation of Eq. (7). The dots stand for the measurements. Each experimental point represents the mean value of the $2n$ angles measured in a n crack pattern. The inserted figure shows the evolution of the global energy U^* with crack number n, computed for penetration radii 2, 4, and 6 mm.

$$\frac{\delta\phi_n}{\delta l} = -\frac{\tan(\pi/n-\phi_n)}{\cos(\pi/n-\phi_n)}\frac{1}{R}, \tag{4}$$

the condition on n and ϕ_n being

$$g_n(\phi_n) = \frac{1-\nu^2}{\pi}\left(\frac{\Gamma}{ER}\right)\frac{R_s^2-R^2}{R^2}\left((1-\nu)\frac{R_s^2}{R^2}+1+\nu\right)^{-1}, \tag{5}$$

in which the function g_n writes as

$$g_n(\phi_n) = \frac{\phi_n \sin(\pi/n-\phi_n)\cos(\pi/n-\phi_n)}{n\sin(\pi/n)\tan(\pi/n-\phi_n)}\epsilon_n. \tag{6}$$

This relation, linking the couples (n, ϕ_n) to the material properties, provides the admissible radial crack morphologies. A simpler form of condition (5) may be obtained in the limit of $R \ll R_s$ and $\phi_n \ll \pi/n$. In such conditions, the asymptotic angle ϕ_n writes

$$\phi_n \simeq f(n)\left(\frac{\Gamma}{ER}\right)^{1/3}, \tag{7}$$

in which

$$f(n) = \left\{2\left(\frac{1+\nu}{\pi}\right)\left(\frac{n\tan(\pi/n)}{\cos(\pi/n)}\right)\right\}^{1/3}. \tag{8}$$

Experimental measurements of ϕ_n are shown on Fig. 3(b) for several values of n. The adjusted parameter of the theoretical curves is the fracture energy Γ, and the value $\Gamma = 110\ \mathrm{kJ\cdot m^{-2}}$ matching well the experimental data is also consistent with the order of magnitude observed in other studies of the petaling of thick aluminum plates [12]. Figure 3(b) shows that the prediction of the angle ϕ_n is in very good agreement with measurements. In addition, the approximated formula (7) (dashed line) works well for small penetration radii R, as expected. We emphasize that the value of the fracture energy Γ obtained above embraces both kind of irreversibilities, namely, surface creation by crack propagation (the surface energy), and plastic strain work at the crack tips.

Thus, Griffith's criterion allows the determination of ϕ_n if n is known. To compute the most probable number of cracks n^*, we minimize the global energy of the system throughout the perforation process, an approach sometimes used to predict crack path in fracture mechanics [13]. Hence, n^* satisfies

$$\frac{\partial}{\partial n}\left(\frac{1}{R-R_c}\int_{R_c}^{R} U dR\right) = \left.\frac{\partial U^*}{\partial n}\right|_{n=n^*} = 0, \tag{9}$$

where R_c is the penetration radius at which cracks appear. The evolution of U^* with n is reported in Fig. 3(a). Theory predicts an optimal number of cracks between $n = 4$ and $n = 5$, consistently with the experimental observations reported in Fig. 2.

To understand the dispersion in the final number of cracks, we consider the discrete nature of the problem. When $n > n^*$, the radial crack pattern should rearrange to reduce the number of cracks from n to $n-1$ by crossing an energy barrier. When a crack stops, in the area of the sheet comprised between the two other adjacent cracks, the strain increases locally to its maximal value as the crack approaches the edge of the cone. Hence the expression of the normalized energy barrier is

$$\frac{\Delta U_e}{U_e} = \frac{\tilde{\epsilon}_n^2 - \epsilon_n^2}{n\epsilon_n^2}. \tag{10}$$

Since the only energy stored in the system is the elastic energy, the relative energy barrier must satisfy $\Delta U_e/U_e < 1$ in order to allow for crack number decrease. Figure 4(b) shows the energy barrier predicted by the model. In the range of parameters of our experiments, the system is able to spontaneously decrease the number of cracks for $n > 10$ only, since $\Delta U_e/U_e > 1$ for smaller n. Moreover, the energy barriers tend to be higher for larger R, thus preventing any rearrangement with increasing penetration depth, as experiments show.

Therefore, both the prediction of the optimal number of cracks n^* and the energy gaps criterion offer a good understanding of the experimental results reported in Fig. 2. In particular, the dispersion of the initial number of cracks $n_0 < 5$ can be interpreted as the signature of initial defects. Indeed, if local imperfections initiate the creation of addi-

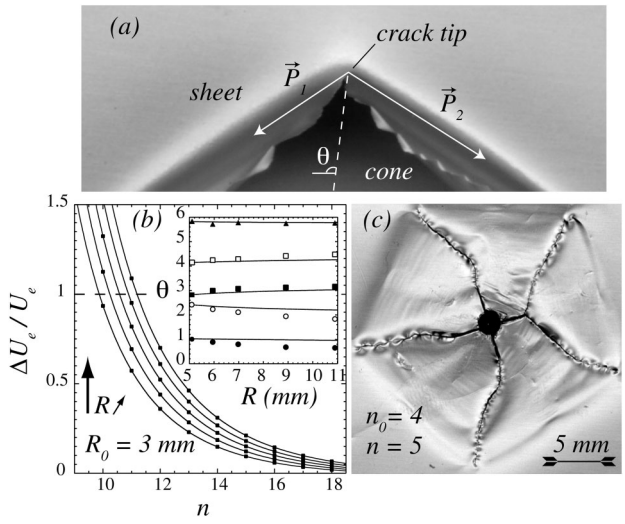

FIG. 4. (a) Sketch of a crack tip in a random pattern. Two punctual forces $\vec{P}_{1,2}$, tangent to the cone, act on the corner formed by the crack tip. (b) Evolution of the switching energy with the crack number n, computed for perforation radii ranging from 10.5 to 12.5 mm. The inserted figure shows the evolution of the angular position of the cracks θ (in radians) with the penetration radius R. The dots stand for measurements and the solid line for theoretical predictions. (c) Post mortem crack path of a perforated aluminum sheet.

tional cracks such that $n > n^*$, although the energy state of the system is not minimized, high energy gaps prevent the crack pattern from reaching the optimal number of cracks n^*. Nevertheless, for a large number of initial cracks, the system relaxes to fewer cracks, typically $n = 10$ in the case of aluminum sheets, as for the other materials we have tested, like paper for instance.

Experiments also show that a random crack distribution systematically evolves toward a regular pattern of cracks expanding radially (with uniform angles). To describe the evolution of the pattern, we refer to the principle of local symmetry which implies the conservation of the local symmetry around a crack tip during its propagation [14]. The symmetry axis of the stress field around a crack in a random pattern deviates from the radial direction and so does the direction of propagation of the crack. We use the solution to the elastic problem of two punctual forces acting on a corner [15] to crudely approximate the stress field around a crack tip, see Fig. 4(a). Then, using the principle of local symmetry, we compute the fracture path for a random crack pattern and compare it to the experiment. Results reported in the inserted graphic of Fig. 4(b) show good agreement between the prediction and observed crack trajectories. Thus, since randomly distributed cracks spontaneously evolve toward uniformity, the choice of a model focusing on uniform radial crack patterns is consistent with the observed and predicted phenomenology.

In conclusion, we have shown that the morphology of cracks on an indented thin sheet can be described by a simple argument balancing stretching elastic energy and fracture energy associated with the crack extension. Global energy minimization allows us to infer the most favorable pattern without relying on the precise description of the local features of the cracks. In particular we do not explicitly account for the singular stress field that develops at the tip of the crack, nor for the transition to a plastic behavior in the sheet. Instead, we use an *ad hoc* fracture energy determined from the pattern shape, whose value is used to compute its later evolution, and the number of cracks, in quantitative agreement with many features of the experiment. The pattern shown on Fig. 4(c) epitomizes this evolution: starting with 4 cracks, the system switches to 5 cracks by crack branching and immediately starts to globally rearrange to reach the preferred uniform (symmetrical) state. An obvious extension of this study is to investigate whether those principles help understanding the more complex case of the radial crack patterns in impacted brittle plates–the common broken window case.

We acknowledge support from the Agence Nationale de la Recherche and the Délégation Générale pour l'Armement.

*nvdb@irphe.univ-mrs.fr
†Also at Institut Universitaire de France, Paris, France.

[1] N. Shinkai, in *Fractography of Glass*, edited by R. C. Bradt and R. E. Tressler (Plenum Press, New York, 1994).
[2] J. Åström and J. Timonen, Phys. Rev. Lett. **79**, 3684 (1997).
[3] Y. Li and Z. P. Bažant, J. Eng. Mech. **120**, 1481 (1994).
[4] B. Landkof and W. Goldsmith, Int. J. Solids Struct. **21**, 245 (1985).
[5] Y. Rhee, H.-W. Kim, Y. Deng, and B. Lawn, J. Am. Ceram. Soc. **84**, 1066 (2001).
[6] G. Gauthier, V. Lazarus, and L. Pauchard, Europhys. Lett. **89**, 26002 (2010).
[7] J. Locke and J. A. Unikowski, Forensic Sci. Int. **51**, 251 (1991).
[8] V. Romero, E. Cerda, and B. Roman (to be published).
[9] B. Audoly, P. M. Reis, and B. Roman, Phys. Rev. Lett. **95**, 025502 (2005).
[10] G. Lamé, *Leçons Sur La Théorie Mathématique De L'élasticité Des Corps Solides* (Gauthiers-Villars, Paris, 1866), p. 188.
[11] A. A. Griffith, Phil. Trans. R. Soc. A **221**, 163 (1921).
[12] K. Kaminishi, M. Taneda, and S. Tanaka, JSME Int. J., Ser. I **35**, 475 (1992).
[13] G. Francfort and J. Marigo, J. Mech. Phys. Solids **46**, 1319 (1998).
[14] R. V. Gol'dstein and R. L. Salganik, Int. J. Fract. **10**, 507 (1974).
[15] S. P. Timoshenko and J. N. Goodier, *Theory of Elasticity* (McGraw-Hill Editions, Singapore, 1970), 3rd ed.